DOI: 10.1534/genetics.106.070300

The Biologically Relevant Targets and Binding Affinity Requirements for the Function of the Yeast Actin-Binding Protein 1 Src-Homology 3 Domain Vary With Genetic Context

Jennifer Haynes,*,† Bianca Garcia,* Elliott J. Stollar,‡,§ Arianna Rath,‡ Brenda J. Andrews*,†,,[1] and Alan R. Davidson*,‡**

**Department of Molecular and Medical Genetics, †Terrence Donnelly Centre for Cellular and Biomolecular Research, ‡Department of Biochemistry, and **Banting and Best Department of Medical Research, University of Toronto, Toronto, Ontario M5S 1A8, Canada and §Structural Biology and Biochemistry, Hospital for Sick Children, Toronto, Ontario M5G 1X8, Canada*

Manuscript received December 26, 2006
Accepted for publication March 2, 2007

ABSTRACT

Many protein–protein interaction domains bind to multiple targets. However, little is known about how the interactions of a single domain with many proteins are controlled and modulated under varying cellular conditions. In this study, we investigated the *in vivo* effects of Abp1p SH3 domain mutants that incrementally reduce target-binding affinity in four different yeast mutant backgrounds in which Abp1p activity is essential for growth. Although the severity of the phenotypic defects observed generally increased as binding affinity was reduced, some genetic backgrounds (*prk1*Δ and *sla1*Δ) tolerated large affinity reductions while others (*sac6*Δ and *sla2*Δ) were much more sensitive to these reductions. To elucidate the mechanisms behind these observations, we determined that Ark1p is the most important Abp1p SH3 domain interactor in *prk1*Δ cells, but that interactions with multiple targets, including Ark1p and Scp1p, are required in the *sac6*Δ background. We establish that the Abp1p SH3 domain makes different, functionally important interactions under different genetic conditions, and these changes in function are reflected by changes in the binding affinity requirement of the domain. These data provide the first evidence of biological relevance for any Abp1p SH3 domain-mediated interaction. We also find that considerable reductions in binding affinity are tolerated by the cell with little effect on growth rate, even when the actin cytoskeletal morphology is significantly perturbed.

TO understand the functioning of cells, it is essential to accurately define the networks of protein–protein interactions that occur within them. To this end, many proteomic studies have aimed to identify large numbers of protein–protein interactions within cells (Gavin *et al.* 2002; Ho *et al.* 2002; Li *et al.* 2004; Rual *et al.* 2005). A confounding finding in these studies is that single proteins or protein domains are often seen to interact with many different targets, sometimes numbering in the dozens. At present, there is little known about how these multiple interactions are regulated and whether crucial interaction targets may change under varying environmental conditions or genetic backgrounds. To address these issues, cellular systems involving multiple protein–protein interactions must be analyzed in quantitative detail. In this study, we systematically investigated the *in vivo* effects of mutations that alter the peptide-binding affinity of the Src-homology 3 (SH3) domain of yeast actin-binding protein 1 (Abp1p).

[1]*Corresponding author*: Terrence Donnelly Centre for Cellular and Biomolecular Research, University of Toronto, 160 College St., Toronto, ON M5S 3E1, Canada. E-mail: brenda.andrews@utoronto.ca

Abp1p is one of a large roster of proteins involved in actin cytoskeleton regulation and endocytosis that colocalize to cortical actin patches (Drubin *et al.* 1988; Mulholland *et al.* 1994). Abp1p was originally identified by actin filament affinity chromatography and was first implicated in regulation of the actin cytoskeleton upon observation that overexpression of *ABP1* causes defects in actin cytoskeleton organization, bud-site selection, and temperature-sensitive growth (Drubin *et al.* 1988). Although deletion of *ABP1* does not cause any readily detectable phenotype, an *abp1*Δ mutant exhibits synthetic genetic interactions with other conserved actin cytoskeleton regulatory genes: *SLA1*, *SLA2*, *SAC6*, and *PRK1* (Holtzman *et al.* 1993; Cope *et al.* 1999). Abp1p is a multidomain protein, capable of interacting with other proteins involved in actin cytoskeleton regulation and endocytosis. At its N terminus, it has an actin-depolymerizing factor/cofilin homology domain that is required for actin filament binding and activation of the Arp2/3 complex *in vitro*, followed by two acidic motifs that are also involved in Arp2/3 activation (Drubin 1990; Cope *et al.* 1999; Goode *et al.* 2001). Abp1p also contains a proline-rich region and a C-terminal SH3 domain, which are required for mediating

protein–protein interactions with other cortical actin patch proteins (Lila and Drubin 1997; Fazi *et al.* 2002; Warren *et al.* 2002; Stefan *et al.* 2005). Homologs of Abp1p in mammalian cells are implicated in processes involving actin rearrangement, such as endocytosis and cell motility (reviewed in Engqvist-Goldstein and Drubin 2003).

Recent detailed live imaging studies of endocytic internalization in yeast have definitively identified cortical actin patches as sites of endocytosis and have classified several protein complexes or modules that dynamically participate in plasma membrane invagination and vesicle scission (Kaksonen *et al.* 2003, 2005; Newpher *et al.* 2005). These modules include several proteins that interact with Abp1p. Endocytic coat proteins, including clathrin, Sla1p, Sla2p, and Pan1p (the "coat module"), are recruited early to endocytic sites at the plasma membrane. Actin polymerization, which is facilitated by actin regulatory proteins, including Abp1p, Sac6p, and the Arp2/3 complex (the "actin module"), drives coat internalization and disassembly. Sla1p and Pan1p are phosphorylated by Ark1p and Prk1p, which are actin patch-localized kinases with partially overlapping functions (Cope *et al.* 1999; Zeng *et al.* 2001). The activity of these kinases is implicated in mediating the disassembly of actin patches after internalization, since in the absence of Ark1p and Prk1p, endocytosis is blocked and actin patches rapidly aggregate into large clumps containing Abp1p, Sla1p, Sla2p, and Pan1p (Cope *et al.* 1999; Sekiya-Kawasaki *et al.* 2003; Toshima *et al.* 2005).

SH3 domains are small (~60 amino acids) conserved protein–protein interaction modules found in a large number of eukaryotic proteins that are involved in cytoskeleton organization and signal transduction pathways (reviewed in Pawson and Scott 1997; Mayer 2001). They bind to short peptides (9–15 amino acids) that usually contain a PxxP core conserved binding motif (where "P" is proline, and "x" can be any amino acid; Ren *et al.* 1993). The SH3 domain of Abp1p is well suited for addressing questions relating to protein domains interacting with multiple binding partners because it has been shown in our laboratory to bind peptides derived from five different cortical actin patch proteins (Ark1p, Prk1p, Srv2p, Sjl2p, and Scp1p) with K_d values ranging from 0.3 to 4.5 μM (Rath and Davidson 2000; our unpublished results). *In vivo*, the Abp1p SH3 domain is required for efficient actin patch localization of at least four of these proteins (Lila and Drubin 1997; Fazi *et al.* 2002; Stefan *et al.* 2005). Furthermore, yeast two-hybrid, phage display, and computational studies suggest that there are other as yet uncharacterized binding targets of this domain (Fazi *et al.* 2002; Landgraf *et al.* 2004; Beltrao and Serrano 2005; Stefan *et al.* 2005). The Abp1p SH3 domain is clearly required for the biological activity of Abp1p as assessed by complementation studies in double mutant strains where Abp1p is required for cell viability (Lila and Drubin 1997); however, it remains unclear which of the many putative interaction partners for the Abp1p SH3 domain may be most important in different genetic conditions.

Accurate modeling of dynamic protein–protein interactions, such as those involved in cell polarity and endocytosis, requires a detailed understanding of the roles of binding affinity and specificity in directing interaction networks. Previous work in our laboratory on the yeast Sho1p SH3 domain demonstrated a strong correlation between changes in the binding affinity of mutants for the biologically relevant target of the domain and quantitated *in vivo* outputs (Marles *et al.* 2004). This study highlighted the importance of the level of binding affinity in determining the function of a protein–protein interaction module. Our studies on Sho1p were interpretable because the measured *in vivo* activity of its SH3 domain results primarily from interaction with a single well-characterized target protein. To date, a similar quantitative *in vitro* and *in vivo* analysis of a domain that possesses multiple biologically relevant targets has not been undertaken.

In this study, we utilize the Abp1p SH3 domain as a model system to address the relationship between binding affinity and biological function for a domain with multiple binding targets. To assess whether the binding affinity requirements for this domain may change under varying conditions, we characterized the effects of affinity-reducing point mutations in four different mutant backgrounds. To provide a mechanistic interpretation of the strain-specific differences that we observed, we also determined the importance of two Abp1p SH3 domain-mediated interactions for viability in two different mutant backgrounds. We definitively demonstrate the biological relevance of Abp1p SH3 domain targets and show that they change under different genetic conditions, a variance that leads to different binding affinity requirements.

MATERIALS AND METHODS

Yeast strains and media: Yeast strains are listed in Table 1. Standard methods and media were used for strain manipulation and growth (Guthrie and Fink 1991). Some strains were obtained from the deletion mutant collection that was constructed by the deletion consortium (Brachmann *et al.* 1998; Winzeler *et al.* 1999). Other strains were made using standard yeast genetic techniques (Guthrie and Fink 1991). All gene disruptions and modifications were achieved by homologous recombination at their chromosomal loci by standard PCR-based methods (Longtine *et al.* 1998). To construct a strain that lacks the polyproline (PP) region of Ark1p (*ark1-ΔPP*), pDD962 was used as a template for PCR-based integration. pDD962 contains sequence that encodes Ark1p-Δ608-626-3Myc, in which amino acids from K608 to P626 are substituted with two A residues (Fazi *et al.* 2002). To construct a strain that lacks the polyproline region of Scp1p (*scp1-PP**), pAG18 was used as a template for PCR-based

TABLE 1

Yeast strains used in this study

Strain	Genotype	Source
BY263[a]	*MAT***a** *trp1Δ63 ura3-52 lys2-801 ade2-107 his3Δ200 leu2-Δ1*	Measday *et al.* (1994)
BY1009[a]	BY263 *abp1Δ::kan*	This study
BY1077[a]	BY448 *ark1Δ::His5*	Friesen *et al.* (2003)
BY1263[a]	BY263 *ARK1-3xHA::TRP1*	This study
BY1266[a]	BY263 *PRK1-3xHA::TRP1*	This study
BY1858[a]	BY263 *abp1Δ::kan ARK1-3xHA::TRP1*	Cross of BY1009 × BY1263
BY1859[a]	BY263 *abp1Δ::kan PRK1-3xHA::TRP1*	Cross of BY1009 × BY1266
BY2916[a]	BY263 *abp1-SH3-N53A::Nat*	This study
BY2917[a]	BY263 *abp1-SH3-Y54A::Nat*	This study
BY2918[a]	BY263 *abp1-ΔSH3::Nat*	This study
BY2987[a]	BY263 *ark1Δ::His5 abp1-SH3-N53A::Nat*	Cross of BY1077 × BY2916
BY2988[a]	BY263 *ark1Δ::His5 abp1-SH3-Y54A::Nat*	Cross of BY1077 × BY2917
BY2989[a]	BY263 *ark1Δ::His5 abp1-ΔSH3::Nat*	Cross of BY1077 × BY2918
BY4741[b]	*MAT***a** *ura3Δ0 leu2Δ0 his3Δ1 met15Δ0*	Brachmann *et al.* (1998)
BY4742[b]	*MATα ura3Δ0 leu2Δ0 his3Δ1 lys2Δ0*	Brachmann *et al.* (1998)
BY2803[b]	BY4741 *sac6Δ::kan*	Deletion consortium
BY2807[b]	BY4741 *sla1Δ::kan*	Deletion consortium
BY2985[b]	BY4741 *prk1Δ::kan*	Deletion consortium
BY2986[b]	BY4741 *sla2Δ::kan*	Deletion consortium
BY1689[b]	*MATα ura3Δ0 leu2Δ0 his3Δ1 lys2Δ0 mfa1Δ::MFA-pr-HIS3 can1Δ0 abp1Δ::Nat*	This study
BY2912[b]	*MATα ura3Δ0 leu2Δ0 his3Δ1 lys2Δ0 mfa1Δ::MFA-pr-HIS3 can1Δ0 abp1-SH3-N53A::Nat*	This study
BY2913[b]	*MATα ura3Δ0 leu2Δ0 his3Δ1 lys2Δ0 mfa1Δ::MFA-pr-HIS3 can1Δ0 abp1-SH3-Y54A::Nat*	This study
BY2914[b]	*MATα ura3Δ0 leu2Δ0 his3Δ1 lys2Δ0 mfa1Δ::MFA-pr-HIS3 can1Δ0 abp1-ΔSH3::Nat*	This study
BY2990[b]	*MAT***a** *ura3 leu2 his3 MFA-pr-HIS3 abp1-SH3-N53A::Nat prk1Δ::kan*	Cross of BY2912 × BY2985
BY2991[b]	*MAT***a** *ura3 leu2 his3 MFA-pr-HIS3 abp1-SH3-Y54A::Nat prk1Δ::kan*	Cross of BY2913 × BY2985
BY2992[b]	*MAT***a** *ura3 leu2 his3 MFA-pr-HIS3 abp1-ΔSH3::Nat prk1Δ::kan*	Cross of BY2914 × BY2985
BY2993[b]	*MAT***a** *ura3 leu2 his3 MFA-pr-HIS3 abp1-SH3-N53A::Nat sla1Δ::kan*	Cross of BY2912 × BY2807
BY2994[b]	*MAT***a** *ura3 leu2 his3 MFA-pr-HIS3 abp1-SH3-Y54A::Nat sla1Δ::kan*	Cross of BY2913 × BY2807
BY2995[b]	*MAT***a** *ura3 leu2 his3 MFA-pr-HIS3 abp1-ΔSH3::Nat sla1Δ::kan*	Cross of BY2914 × BY2807
BY2996[b]	*MAT***a** *ura3 leu2 his3 MFA-pr-HIS3 abp1-SH3-N53A::Nat sac6Δ::kan*	Cross of BY2912 × BY2803
BY2997[b]	*MAT***a** *ura3 leu2 his3 MFA-pr-HIS3 abp1-SH3-Y54A::Nat sac6Δ::kan*	Cross of BY2913 × BY2803
BY2998[b]	*MAT***a** *ura3 leu2 his3 MFA-pr-HIS3 abp1-ΔSH3::Nat sac6Δ::kan*	Cross of BY2914 × BY2803
BY2999[b]	*MAT***a** *ura3 leu2 his3 MFA-pr-HIS3 abp1-SH3-N53A::Nat sla2Δ::kan*	Cross of BY2912 × BY2986
BY3000[b]	*MAT***a** *ura3 leu2 his3 MFA-pr-HIS3 abp1-SH3-Y54A::Nat sla2Δ::kan*	Cross of BY2913 × BY2986
BY3001[b]	*MAT***a** *ura3 leu2 his3 MFA-pr-HIS3 abp1-ΔSH3::Nat sla2Δ::kan*	Cross of BY2914 × BY2986
BY3070[b]	*MATα ura3Δ0 leu2Δ0 his3Δ1 lys2Δ0 mfa1Δ::MFA-pr-HIS3 can1Δ0 abp1-SH3-Y54V::Nat*	This study
BY3071[b]	*MATα ura3Δ0 leu2Δ0 his3Δ1 lys2Δ0 mfa1Δ::MFA-pr-HIS3 can1Δ0 abp1-SH3-Y54P::Nat*	This study
BY3072[b]	*MAT***a** *ura3 leu2 his3 MFA-pr-HIS3 abp1-SH3-Y54V::Nat prk1Δ::kan*	Cross of BY3070 × BY2985
BY3073[b]	*MAT***a** *ura3 leu2 his3 MFA-pr-HIS3 abp1-SH3-Y54P::Nat prk1Δ::kan*	Cross of BY3071 × BY2985
BY4007[b]	*MAT***a** *ura3 leu2 his3 MFA-pr-HIS3 abp1-SH3-Y54V::Nat sac6Δ::kan*	Cross of BY3070 × BY2803
BY4008[b]	*MAT***a** *ura3 leu2 his3 MFA-pr-HIS3 abp1-SH3-Y54P::Nat sac6Δ::kan*	Cross of BY3071 × BY2803
BY4022	*MAT***a** *lys2 leu2 ura3 his3 bar1 end4::HIS3 end4-Δ376-501:TRP1 abp1::URA3*	Wesp *et al.* (1997)
BY4070[b]	BY4742 *ark1-Δ608-626-3xMyc::Hph*	This study
BY4075[b]	*MAT***a** *ura3 leu2 his3 ark1-Δ608-626-3xMyc::Hph prk1Δ::kan*	Cross of BY4070 × BY2985
BY4080[b]	BY4742 *scp1-P156A,P159A::Hph*	This study
BY4081[b]	*MAT***a** *ura3 leu2 his3 lys2 scp1-P156A,P159A::Hph abp1-SH3-Y54A::Nat*	Cross of BY4080 × BY2913
BY4082[b]	*MAT***a** *ura3 leu2 his3 lys2 scp1-P156A,P159A::Hph abp1Δ-SH3::Nat*	Cross of BY4080 × BY2914
BY4083[b]	*MAT***a** *ura3 leu2 his3 scp1-P156A,P159A::Hph prk1Δ::kan*	Cross of BY4080 × BY2985
BY4084[b]	*MAT***a** *ura3 leu2 his3 scp1-P156A,P159A::Hph prk1Δ::kan abp1-SH3-Y54A::Nat*	Cross of BY4080 × BY2991
BY4085[b]	*MAT***a** *ura3 leu2 his3 scp1-P156A,P159A::Hph prk1Δ::kan abp1Δ-SH3::Nat*	Cross of BY4080 × BY2992
BY4118[b]	*MAT***a** *ura3 leu2 his3 lys2 scp1-P156A,P159A::Hph abp1-SH3-Y54V::Nat*	Cross of BY4080 × BY3070
BY4119[b]	*MAT***a** *ura3 leu2 his3 ark1-Δ608-626-3xMyc::Hph sac6Δ::kan*	Cross of BY4070 × BY2803
BY4120[b]	*MAT***a** *ura3 leu2 his3 ark1-Δ608-626-3xMyc::Hph sac6Δ::kan abp1-SH3-Y54V::Nat*	Cross of BY4070 × BY4007
BY4021[b]	*MAT***a** *ura3 leu2 his3 scp1-P156A,P159A::Hph sac6Δ::kan*	Cross of BY4080 × BY2803
BY4022[b]	*MAT***a** *ura3 leu2 his3 scp1-P156A,P159A::Hph sac6Δ::kan abp1-SH3-Y54V::Nat*	Cross of BY4080 × BY4007
BY4142[b]	BY4742 *ark1-Δ608-626-3xMyc::Hph scp1-P156A,P159A::Hph*	Cross of BY4070 × BY4080
BY4143[b]	*MAT***a** *ura3 leu2 his3 lys2 ark1-Δ608-626-3xMyc::Hph scp1-P156A, P159A::Hph sac6Δ::kan abp1-SH3-Y54V::Nat*	Cross of BY4142 × BY2803

[a] Strains are isogenic to the parent strain, BY263, an S288C derivative.
[b] Strains from the deletion consortium are isogenic to the parent strain, BY4741, also an S288C derivative.

TABLE 2

Plasmids used in this study

Plasmid	Description	Source
pABP1-SH3	Codons 535-592 of *ABP1* were PCR amplified and subcloned into pET-21d+ (Novagen, Madison, WI) to give *ABP1* SH3 with a C-terminal 6-His tag under the control of the T7 promoter.	Rath and Davidson (2000)
pABP1-SH3-N53A	pABP1-SH3 derivative containing *ABP1* SH3 with the N53A substitution	This study
pABP1-SH3-Y54A	pABP1-SH3 derivative containing *ABP1* SH3 with the Y54A substitution	This study
pABP1-SH3-Y54V	pABP1-SH3 derivative containing *ABP1* SH3 with the Y54V substitution	This study
pABP1-SH3-Y54P	pABP1-SH3 derivative containing *ABP1* SH3 with the Y54P substitution	This study
pGST-SRV2-CTR	Contains C-terminal *SRV2* coding sequence (codons 253–526), including the K325A and K326A substitutions, fused to the C-terminus of GST; allows for expression of GST-Srv2-CTR in bacteria.	Mattila *et al.* (2004)
pGAL-ARK1-GFP	Contains *ARK1* coding sequence, including the kinase dead K56A substitution, fused to the N terminus of GFP (wild type); allows for expression of Ark1-GFP under the inducible *GAL1,10* promoter.	Cope *et al.* (1999)
p316Δ*Sal*I-ABP1	A 3.5-kb fragment containing the *ABP1* ORF plus 1.5 kb upstream and 180 bp downstream was subcloned into p316 Δ*Sal*I	This study
p316Δ*Sal*I-ABP1-ΔSH3	p316Δ*Sal*I-ABP1 derivative containing *ABP1* with the SH3 domain deletion	This study
p316Δ*Sal*I-ABP1-SH3-N53A	p316Δ*Sal*I-ABP1 derivative containing *ABP1* SH3 with the N53A substitution	This study
p316Δ*Sal*I-ABP1-SH3-Y54A	p316Δ*Sal*I-ABP1 derivative containing *ABP1* SH3 with the Y54A substitution	This study
p316Δ*Sal*I-ABP1-SH3-Y54V	p316Δ*Sal*I-ABP1 derivative containing *ABP1* SH3 with the Y54V substitution	This study
p316Δ*Sal*I-ABP1-SH3-Y54P	p316Δ*Sal*I-ABP1 derivative containing *ABP1* SH3 with the Y54P substitution	This study
p315-ABP1	A 3.5-kb fragment containing the *ABP1* ORF plus 1.5 kb upstream and 180 bp downstream was subcloned into pRS315.	This study
p315-ABP1-ΔSH3	p315-ABP1 derivative containing *ABP1* with the SH3 domain deletion	This study
p315-ABP1-SH3-Y54A	p315-ABP1 derivative containing *ABP1* SH3 with the Y54A substitution	This study

integration. pAG18 contains sequence that encodes Scp1p, in which amino acids P156 and P159 are changed to A residues (kind gift from A. Goodman and B. Goode). Standard rich medium with glucose [yeast extract–peptone–dextrose (YPD)] was used for growing yeast strains. Minimal medium [synthetic dextrose (SD)] was supplemented with appropriate amino acids for plasmid maintenance and with caffeine (3 mm) to create stress conditions. Synthetic medium used for galactose-induction conditions was supplemented with 2% galactose (G) and 2% raffinose (R) instead of dextrose.

Plasmid construction: Plasmids are described in Table 2. Bacterial expression plasmids for Abp1p-SH3-N53A and Abp1p-SH3-Y54A were constructed as previously described (Rath and Davidson 2000). Bacterial expression plasmids for Abp1p-SH3-Y54* were also constructed by this method, but with p316Δ*Sal*I-ABP1-SH3-Y54* templates (*, V or P).

Yeast expression plasmids for Abp1p SH3 domain mutants were constructed and subsequently used as template DNA for PCR-based integration of *ABP1* alleles. To construct an *ABP1* yeast expression plasmid, a 3.5-kb *Eco*RI fragment containing *ABP1* from pDD3 (Lila and Drubin 1997) was subcloned into the *Eco*RI site of p316Δ*Sal*I. To create p316Δ*Sal*I, pRS316 (Sikorski and Hieter 1989) was linearized with *Sal*I, treated with T7 DNA polymerase to remove 3′-overhangs (New England Biolabs, Beverly, MA), and religated.

To construct an *ABP1-ΔSH3* yeast expression plasmid, *NATMX* was amplified using primers (5′-**TGCAGCTCCTCCTCCGCCTCCAAGACGAGCAACTCCAGAGAAAAAGCCAAAGGAA**TAGTCGACATGGAGGCCCAAGAATACCC-3′ and 5′-**TGTAAGTATTTTTTTACGTAAGAATAATATAATAGCATGACGCTGACGTGTGATT**GTCGACCAGTATAGCGACCAGCATTCAC-3′), which anneal to *NATMX* and contain *ABP1* sequences that flank the SH3 domain (in boldface type) and introduce *Sal*I sites, with p4339 as the template (Tong *et al.* 2001). PCR product and *Sal*I-linearized p316Δ*Sal*I-ABP1 were transformed into BY1009 (Table 1) and recombinant plasmid was recovered from Ura+ *natR* transformants that expressed Abp1p-ΔSH3. The plasmid was digested with *Sal*I and religated to remove a 1.3-kb fragment containing *NATMX* sequence.

To construct *ABP1-SH3-N53A* and *ABP1-SH3-Y54** yeast expression plasmids, *ABP1 SH3* sequence was amplified using primers [5′-**CTCCTCCGCCTCCAAGACGAGCAACTCCAGAGAAAAAGCCAAAGGAA**AATCCTTGGGCCACAGCAG-3′ and 5′-**TTTTTTACGTAAGAATAATATAATAGCATGACGCTGACGTGTGATT**CTAGTTGCCCAAAGACACATAATTGC-3′ (N53A) or 5′-**TTTTTTACGTAAGAATAATATAATAGCATGACGCTGACGTGTGATT**CTAGTTGCCCAAAGACACYRBATTGC-3′ (Y54*; Y, C/T; R, A/G; B, G/C/T)], which anneal to *ABP1 SH3* sequence and contain *ABP1* sequences that flank the SH3 domain (in boldface type), with pABP1-SH3 bacterial expression plasmids as the template. PCR product and *Sal*I-linearized p316Δ*Sal*I-ABP1-ΔSH3 were transformed into BY1009, and recombinant plasmid was recovered from Ura+ transformants that expressed Abp1p. PCR reactions were done using Platinum *Pfx* DNA polymerase (Invitrogen, San Diego) as recommended by the manufacturer. The integrity of all PCR-amplified DNA was confirmed by sequencing.

Protein purification: Abp1p SH3 domains were expressed in *Escherichia coli* BL21 STAR (λDE3) (Novagen), which contains a deletion of the RNaseE gene (*rne131*) to increase protein expression levels. Cells were grown to an OD_{600} of 0.6–0.8 and induced with 1 mm IPTG for 3 hr. All Abp1p SH3 domain purifications were carried out in 6 m GuHCl using Ni-NTA (QIAGEN, Chatsworth, CA) affinity chromatography as previously described (Rath and Davidson 2000). Once purified, proteins were refolded by dialysis into the appropriate buffer (see below).

GST-Srv2p-CTR (Mattila *et al.* 2004) was purified from a 50-ml culture of *E. coli* as previously described (Measday *et al.* 1997). GST-Srv2p-CTR concentration was approximated by comparison of purified protein aliquots to BSA standards (Sigma, St. Louis) on a Coomassie Blue-stained 8% SDS–polyacrylamide gel.

***In vitro* peptide binding and protein stability assays:** Seventeen-residue target peptides derived from *ARK1* (KKTKPTPPPKPSHLKPK), *SRV2* (KSGPPPRPKKPSTLKTK), and *SCP1* (KKPRPPVKSKPKHLQDG) were synthesized and amidated on the C terminus (Biomer Technology). Peptides were purified by reverse-phase chromatography using a C-18 column. To avoid heat signals from the mixing of nonequivalent buffers, Abp1p SH3 domains and the peptide samples were dialyzed into 50 mm sodium phosphate (pH 7.0), 100 mm NaCl, using MWCO 500 membrane tubing (SpectraPor). The concentration of Abp1p SH3 domains was determined spectrophotometrically using a molar extinction coefficient at 280 nm = 20.91 mM^{-1} cm^{-1} (19.6 mM^{-1} cm^{-1} for Y54 mutants). The concentration of the peptides was determined using amino acid analysis (Hospital for Sick Children).

In vitro peptide-binding assays were performed by *i*sothermal *t*itration *c*alorimetry (ITC) at 30°, using a VP-ITC instrument from MicroCal (Northampton, MA). Peptide samples (between 200 and 1000 μM) were individually titrated into SH3 domain samples (between 20 and 100 μM) using a 250-μl syringe, with each titration consisting of 28 × 10-μl injections. Injections were separated by 3-min intervals, and the filter period for data collection was 2 sec. The heat associated with each injection was obtained by integrating the area under the resulting peak using Origin ITC data analysis software (OriginLab; provided with the instrument). Heats of dilution and injection were measured in control experiments in which the SH3 domain or peptide samples were titrated into dialysis buffer. These heats were found to be similar to those observed at the end of the SH3 domain–peptide titrations. The integrated heats from the SH3 domain–peptide experiments were corrected by the enthalpy changes observed at the end of the titrations. The data were analyzed to obtain estimates of the observed dissociation constant (K_d), stoichiometry constant (stoichiometry was 1:1 for mutants tested), and enthalpy of binding using the "single set of identical sites" model within the Origin software package. Experiments were repeated at least three times to also include reverse titrations.

Affinity columns and Western blot analysis: Purified Abp1p SH3 domains were dialyzed into 20 mm HEPES (pH 8.0), 300 mm NaCl, and 10% glycerol and subsequently bound to Affi-Gel 10 resin (Bio-Rad, Hercules, CA) as previously described (Friesen *et al.* 2005). The efficiency of the coupling reaction was determined by comparison of the supernatant before and after coupling, which was measured by Bradford assay and also visualized by 15% Tris–Tricine PAGE and subsequent Coomassie Blue staining of the polyacrylamide gel. The concentration of coupled SH3 domain on the resin was 1.4 μg/μl. Abp1p SH3 domain affinity columns were constructed as previously described (Friesen *et al.* 2005).

Yeast strains (BY1858 and BY1859) were grown in YPD at 30° to midlog phase (OD_{600} ~0.5). Cultures (400 ml) were collected and cells were pelleted by centrifugation. Protein extracts were prepared by lysing cells with glass beads, as previously described (Lee *et al.* 1998). Abp1p SH3 domain affinity resin was incubated with 0.4, 0.8, or 1.6 mg of whole-cell extract and lysis buffer [100 mm Tris–HCl (pH 7.9), 250 mm NaCl, 5 mm EDTA, 50 mm NaF, 0.1% NP-40, 1 mm DTT, 10% glycerol, 1 EDTA-free protease inhibitor cocktail tablet (Boehringer Mannheim, Indianapolis) per 10 ml] to a total volume of 100 μl. Columns were washed twice with 100 μl wash buffer [100 mm Tris–HCl (pH 7.9), 250 mm NaCl, 5 mm EDTA, 0.1% NP-40, 1 mm DTT, 10% glycerol], and bound proteins were eluted with 20 μl SDS elution buffer [100 mm Tris–HCl (pH 7.9), 10% glycerol, 1% SDS], to which 5 μl of 5× SDS sample buffer were added. Total protein eluates were loaded onto a 6% SDS–polyacrylamide gel.

For affinity chromatography with GST-Srv2p-CTR, Abp1p SH3 domain affinity resin was incubated with 3, 6, or 12 μg of GST-Srv2p-CTR and binding buffer [100 mm Tris–HCl (pH 7.0), 250 mm NaCl, 5 mm EDTA, 0.2% Triton X-100, 1 mm DTT, 10% glycerol] to a total volume of 100 μl. Columns were washed twice with 100 μl binding buffer, and bound proteins were eluted with 50 μl SDS elution buffer to which 50 μl of 2× SDS sample buffer were added. Ten percent of the total protein eluates were loaded onto an 8% SDS–polyacrylamide gel. Protein eluates were separated by SDS–PAGE and transferred to nitrocellulose membranes. Proteins were detected by Western blotting with monoclonal anti-HA (F-7) or anti-GST (B-14) antibodies (Santa Cruz Biotech) and detected using enhanced chemiluminescence.

For anti-Abp1p and anti-Swi6p Western blots, strains were grown in YPD+1M sorbitol at room temperature to saturation and then diluted into fresh YPD and grown for 7 hr at room temperature (BY2803, BY2986, BY2997, BY2998, BY3000, BY3001, BY4007, and BY4008), or for 2 hr at room temperature and then shifted to 30° (BY2807, BY2994, and BY2995) or to 37° (BY2985, BY2991, BY2992, BY3072, and BY3073) for 5 hr to midlog phase (OD_{600} ~0.5). Cultures (25 ml) were collected and cells were pelleted by centrifugation. Protein extracts were prepared by lysing cells with glass beads, as previously described (Lee *et al.* 1998). Equal amounts (20 μg) of total protein extract in 1× SDS sample buffer were separated by 8% SDS–PAGE and transferred to nitrocellulose membranes. Proteins were detected by Western blotting with polyclonal anti-Swi6p antibody (Ogas *et al.* 1991) and by using enhanced chemiluminescence. Membranes were stripped of anti-Swi6p antibody and reprobed with polyclonal anti-Abp1p antibody (kind gift from B. Goode). Protein extracts prepared from yeast strains that were sick or dying yield an overall reduction in protein levels, possibly due to cell lysis prior to extract preparation.

Growth assays: To assay growth of strains that carried integrated *ABP1* alleles, cells were grown in YPD+1M sorbitol at room temperature to saturation and then diluted into fresh YPD and grown at room temperature to midlog phase. Serial dilutions were spotted onto SD complete (SC) plates in the absence or presence of 3 mm caffeine (Sigma) and incubated for 3 days at 30° (BY4741, BY2803, BY2807, BY2986, BY2913, BY2914, BY2994, BY2995, BY2997, BY2998, BY3000, BY3001, BY3070, BY4007, BY4008, BY4118, BY4119, BY4120, BY4121, BY4122, BY4142, and BY4143) or at 37° (BY4741, BY2913, BY2914, BY2985, BY2991, BY2992, BY3070, BY3072, BY3073, BY4070, BY4075, BY4080, BY4081, BY4082, BY4083, BY4084, and BY4085).

To assay growth of strains that expressed Abp1p SH3 domain mutants from plasmids, p315-ABP1-SH3 plasmids were individually transformed into the haploid double mutant strain (BY4022). Transformants were grown in SD–Leu at room temperature to saturation and then diluted into fresh SD–Leu and grown at room temperature to midlog phase. Serial dilutions were spotted onto SD–Leu plates in the absence or presence of 3 mm caffeine (Sigma) and incubated for 3 days at 37°.

GFP localization and actin staining: For Ark1p-GFP localization experiments, the galactose-inducible expression plasmid, pGAL-ARK1-GFP (Cope *et al.* 1999), was transformed into strains BY1077, BY2987, BY2988, and BY2989. Transformants were grown in SD–Ura at 30° to saturation and then diluted

into SGR–Ura and grown for 14 hr at 30° to midlog phase. Cells were pelleted and concentrated 10-fold.

For rhodamine–phalloidin staining of filamentous actin, strains were grown in YPD at room temperature to saturation and then diluted into 5 ml fresh YPD and grown for 2 hr at room temperature and then shifted to 37° for 5 hr to midlog phase. Cells were fixed by addition of formaldehyde to the medium to a final concentration of 3.7% for 1.5 hr. Cells were then pelleted, transferred to Eppendorf tubes, washed twice with 1 ml PBS, and resuspended in 100 μl PBS. To stain filamentous actin, 36 μl cell suspensions were incubated for 1.5 hr at room temperature with 4 μl rhodamine-conjugated phalloidin (Molecular Probes, Eugene, OR; 300 units in 1.5 ml methanol) and 0.5 μl 10% Triton X-100, with gentle vortexing every 15 min. Cells were washed three times with 500 μl PBS and resuspended in 25 μl PBS, to which an equal volume of Pro-long antifade reagent (Molecular Probes) was added. Four microliters of each preparation were spotted onto slides and set at room temperature for at least 3 hr before visualization.

Fluorescence microscopy: Strains were examined using phase-contrast microscopy and viewed through either a GFP filter or a rhodamine filter to observe fluorescence at a magnification of ×1000. Photographs were taken with a Roper Scientific CoolSNAP HQ cooled CCD camera (Tucson, AZ) mounted on a Leica DM-LB microscope. Images were analyzed using MetaVue software (Universal Imaging, Media, PA).

RESULTS

***In vitro* binding activity of Abp1p SH3 domain derivatives with binding surface substitutions:** To explore the binding affinity requirements for the *in vivo* activity of the Abp1p SH3 domain, we aimed to create a set of mutants with varying binding affinities for relevant target peptides. For this purpose, we made amino acid substitutions at two positions in the SH3 domain, Asn53 and Tyr54, that were predicted from examination of structures of other SH3 domain-target peptide complexes to make direct contact with the PxxP-containing target peptide (Figure 1A, Note that the numbering system that we use here is for the SH3 domain only and follows the SH3 domain numbering system of Larson and Davidson (2000); residue 1 of the SH3 domain is residue 534 of the full-length Abp1p (Fazi *et al.* 2002; Larson and Davidson 2000). Tyr54 is a conserved aromatic residue that contributes to the formation of one of the hydrophobic binding pockets in the SH3 domain, while Asn53 is a somewhat less conserved residue that makes a hydrogen bond with the backbone of target peptides. We expected that mutations at the Tyr54 position would have larger effects than those at Asn53.

Asn53 and Tyr54 were each individually substituted with Ala, and Tyr54 was also changed to Pro and Val. Each mutant SH3 domain was expressed and purified from *E. coli* as a 6-His fusion and its affinity for target peptides was quantitated by isothermal titration calorimetry. PxxP-containing target peptide sequences were derived from two proteins known to bind the Abp1p SH3 domain *in vivo* and *in vitro*, Ark1p and Srv2p. These sequences matched the extended consensus binding

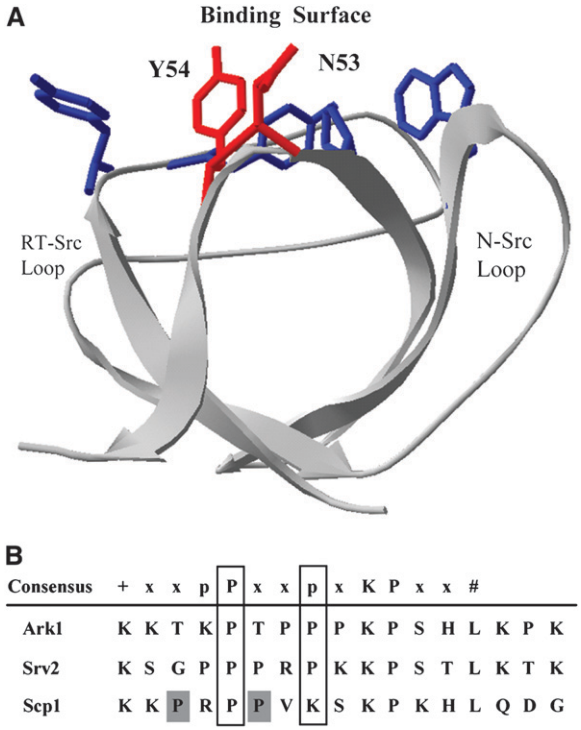

Figure 1.—Abp1p SH3 domain structure and target peptide sequences. (A) The structure of Abp1p SH3 domain (PDB ID, 1JO8; Fazi *et al.* 2002). Residues that were mutated in the Abp1p SH3 domain are in red. Other conserved residues that are important for binding are in blue. (B) PxxP-containing target peptides used for *in vitro* binding assays. The proline residues of the PxxP motif are boxed. The proline residues of a possible alternative PxxP motif in the Scp1p peptide are shaded. The consensus sequence shown here, in which "+" denotes a positively charged residue and "#" denotes a hydrophobic residue, was determined by Fazi *et al.* (2002).

sequence for the Abp1p SH3 domain that was deduced from phage display experiments (Figure 1B; Fazi *et al.* 2002). We chose to investigate binding of the Abp1p SH3 domain mutants to three different target peptides (Figure 1B) as a means to assess whether the magnitude of the effects of mutations might vary depending on the target tested. The Ark1p and Srv2p peptides were chosen for use in our assays because they were the strongest and the weakest binding of the peptides that we have tested in our laboratory (we have also performed assays with peptides derived from Prk1p, Sjl2p, and Scp1p). We performed assays with a PxxP-containing peptide from Scp1p because we discovered that interaction between this protein and the Abp1p SH3 domain is functionally important (see below).

As expected, the Tyr54 mutations caused a marked increase in the dissociation constant (K_d) values of the Abp1p SH3 domain for all of the peptides (Table 3). For example, the Y54A mutant decreased binding affinity for the Ark1p peptide >50-fold. In contrast, the Abp1p SH3 domain carrying the N53A mutation showed considerably smaller effects on binding affinity with

TABLE 3

***In vitro* binding data for Abp1p SH3 domain mutants**

Abp1p SH3 protein	Peptide binding [K_d (μM)][a]			T_m (°C)[b]
	Ark1	Srv2	Scp1	
Wild type	0.27 ± 0.02	4.43 ± 0.4	1 ± 0.05	57
N53A	1.12 ± 0.06	5.56 ± 0.47	NT	62
Y54V	5.67 ± 0.3	16.1 ± 1.73	6.7 ± 2.3	55
Y54A	15.3 ± 1.2	>50[c]	7.2 ± 1.9	57
Y54P	>50[c]	NT	NT	30

NT, not tested.
[a] Determined by isothermal titration calorimetry.
[b] Determined by *in vitro* thermal unfolding experiments.
[c] Binding was not detected; an interaction with a K_d of $< \sim 50$ μM is detectable in this assay.

no significant effect on binding affinity for the Srv2p peptide (1.3-fold) and an increase in K_d for the Ark1p peptide of 4-fold. Overall, this selection of mutants displayed a wide range of K_d values, which was the goal of our mutagenesis strategy. Interestingly, the degree of affinity reduction caused by the mutations depended upon which peptide was being tested. On average, the mutations tested caused an ~5-fold greater reduction in binding affinity when the Ark1p peptide was used in the assay than when the Srv2p peptide was used. We note that the Ark1p protein contains two closely juxtaposed PxxP motifs, and a peptide encompassing the full site containing both motifs bound with exactly the same affinity as the single site (data not shown). It is also noteworthy that mutations affected binding to the Ark1p peptide to a much greater degree even though the wild-type domain binds this peptide much more strongly. The Scp1p peptide appeared to be the least sensitive to mutations in the SH3 domain in that the Y54A mutant displayed only a 7-fold reduction in affinity to this peptide and the Y54A and Y54V mutants displayed similar affinities (Table 3). The distinctive behavior of the Scp1p peptide may be due to its use of an alternative PxxP motif that does not align with those in the other two target peptides.

To ensure that changes in binding affinity were not due to thermodynamic destabilization of the domain itself, we performed *in vitro* thermal unfolding experiments on each mutant in isolation, monitored by circular dichroism spectroscopy. The temperature midpoint of unfolding transition (T_m) of all of the mutants except Y54P was similar to that of the wild-type Abp1p SH3 domain (Table 3). The significant destabilization of the Y54P mutant may be partially responsible for its lack of peptide binding.

Binding of Abp1p SH3 domain mutants to full-length target proteins: We next tested the effects of changes in Abp1p SH3 domain binding affinity in binding assays with full-length target proteins in yeast extracts. For these assays, we used a subset of our Abp1p

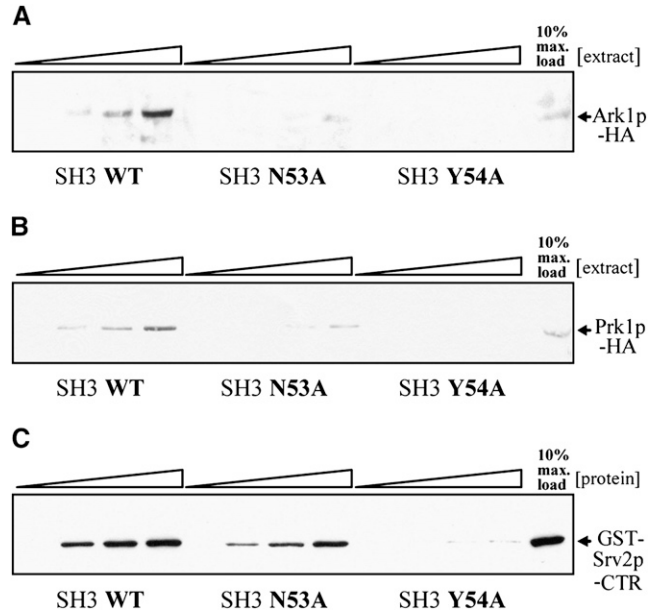

FIGURE 2.—Western blot analysis of target proteins bound to Abp1p SH3 domain affinity resin. Affinity chromatography using wild-type Abp1p SH3 domain (SH3 wild type), a mutant Abp1p SH3 domain with an N53A substitution (SH3 N53A), and a second mutant with a Y54A substitution (SH3 Y54A) as ligands. Increasing amounts of whole-cell extract (0.4, 0.8, and 1.6 mg) from wild-type log-phase cells expressing an HA-epitope-tagged version of either Abp1p SH3 target protein Ark1p (A) or Prk1p (B) were passed over the columns. Columns were washed; and bound proteins were eluted in buffer containing 1% SDS. Eluates were analyzed by Western blotting, using a monoclonal anti-HA antibody. (C) Affinity chromatography using Abp1p SH3 domain ligands described above and increasing amounts of purified GST-Srv2p-CTR protein (3, 6, and 12 μg). Columns were washed and bound proteins were eluted in buffer containing 1% SDS. Ten percent of the eluates were analyzed by Western blotting, using a monoclonal anti-GST antibody. The binding of GST-Srv2p-CTR to the SH3 Y54A column is the same as the binding of GST-Srv2p-CTR to resin alone (data not shown). Max., maximum.

SH3 domain-binding surface mutants, Y54A and N53A, which exhibited large and small *in vitro* binding defects, respectively. Previous work has shown that purified GST-Abp1-SH3 binds Ark1p and Prk1p from yeast extracts and that these interactions require both an intact SH3 domain and poly-proline sequences in the target proteins (Fazi *et al.* 2002). We used Abp1p SH3 domain affinity columns to bind Ark1p fused to a C-terminal 3HA tag from yeast extracts. These assays were performed using *abp1*Δ strains to allow all potential target protein available to bind Abp1p SH3 domain affinity columns. As expected, wild-type Abp1p SH3 domain efficiently bound Ark1p-3HA (Figure 2A). However, Abp1p-SH3-N53A showed reduced binding to Ark1p-3HA, and Abp1p-SH3-Y54A showed no detectable binding to Ark1p-3HA in this assay. Similar results were obtained for Abp1p SH3 domain mutants with Prk1p tagged with 3HA at the C terminus (Figure 2B). These

experiments demonstrate that the changes in affinity that we measured *in vitro* using purified short target peptides are consistent with assays in which binding to full-length target proteins in yeast extract is measured. It is striking that even the relatively small *in vitro* effects of the N53A mutant are accurately reflected in these affinity chromatography experiments. For example, the amount of Ark1p bound to the N53A mutant column loaded with 1.6 mg of whole-cell extract is similar to the amount bound by the wild-type SH3 domain column loaded with 0.4 mg of whole-cell extract, which is expected, given the fourfold decrease in affinity seen for the N53A mutant as measured *in vitro*.

We also attempted to use Abp1p SH3 domain affinity columns to test the effects of changes in Abp1p SH3 domain-binding affinity for the Srv2p target peptide in the context of the native protein. However, since we found that epitope-tagged Srv2p from yeast extracts bound the resin alone in our binding assays, we used the recombinant Srv2p C-terminal region (CTR) expressed as a GST-fusion protein and purified from bacteria. GST-Srv2p-CTR spans amino acids 253–526 of full-length Srv2p and includes the actin-binding region of Srv2p in addition to the proline-rich region to which the Abp1p SH3 domain binds (Lila and Drubin 1997). Both wild-type Abp1p SH3 domain and Abp1p-SH3-N53A efficiently bound GST-Srv2p-CTR (Figure 2C). However, Abp1p-SH3-Y54A did not bind GST-Srv2p-CTR above background levels. These assays provided confirmation of our *in vitro* results with the Srv2p peptide and also demonstrated that the N53A affinity column was competent for efficient peptide binding when given a target at high concentration.

Target protein localization in cells expressing Abp1p SH3 domain mutants: To determine whether Abp1p SH3 domain mutants with reduced affinity for target peptides would elicit a detectable *in vivo* phenotype, we monitored the localization of GFP-tagged Ark1p in yeast strains expressing full-length Abp1p with SH3 domain substitutions. It should be noted that the mutant versions of *ABP1* used in these and other assays described below were integrated into the *ABP1* locus in the yeast genome, so that the mutant alleles were expressed at the normal level from the endogenous *ABP1* promoter. Ark1p and Prk1p localize to cortical actin patches and this localization is dependent upon the Abp1p SH3 domain (Cope *et al.* 1999; Fazi *et al.* 2002). In our experiments, we used a kinase dead version of Ark1p-GFP since elevated levels of Ark1p disrupt normal cortical actin patch morphology and cause abnormal budding and cell death (Cope *et al.* 1999). As expected, in yeast strains that expressed wild-type Abp1p, Ark1p-GFP displayed a punctate localization pattern that is consistent with cortical actin patch localization (Figure 3; note that punctate staining is enriched in the bud of small-budded cells, but does not completely overlap with cortical actin patches in medium- to large-budded cells, consistent with previous observations). In contrast, strains that expressed Abp1p bearing SH3 domain-binding surface substitutions displayed an aberrant localization pattern for Ark1p-GFP. Strains that expressed Abp1p with the Y54A SH3 domain substitution showed a diffuse localization pattern for Ark1p-GFP, similar to Ark1p-GFP localization mediated by Abp1p lacking its SH3 domain. Although strains that expressed Abp1p carrying the N53A SH3 domain substitution still exhibited punctate localization of Ark1p-GFP, the intensity and number of spots was dramatically reduced in these cells. Rhodamine–phalloidin staining of fixed cells showed that the actin cytoskeleton was intact in all strains examined (data not shown). We were unable to test if Abp1p SH3 domain-binding surface mutants affect the *in vivo* localization of Srv2p under the same experimental conditions since overexpression caused aggregation of GFP-Srv2p into a single large bright-staining spot within the cell. Nonetheless, we can conclude from these experiments that even a relatively small reduction of Abp1p SH3 domain-binding affinity, such as that caused by the N53A substitution, leads to an easily detected *in vivo* phenotype as reflected in altered localization of Ark1p. Furthermore, the more dramatic changes in localization observed when Abp1p bearing the Y54A SH3 domain substitution

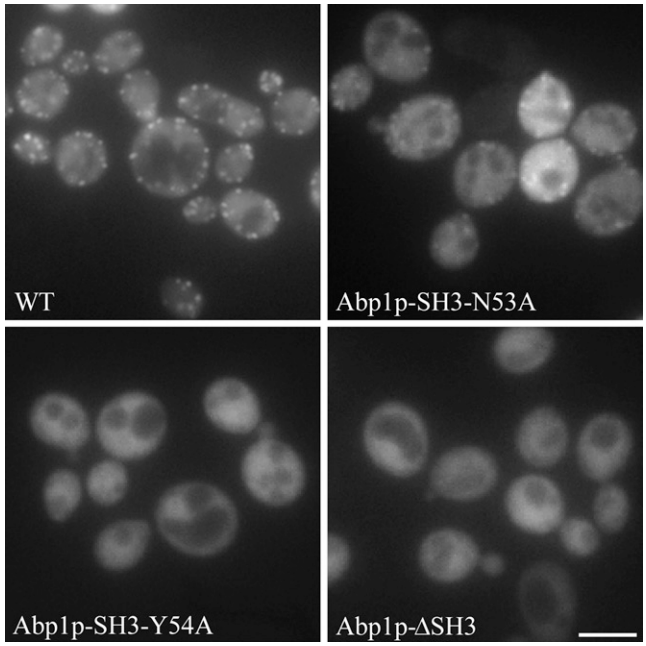

Figure 3.—Localization of Ark1p-GFP in yeast strains expressing wild-type Abp1p or Abp1p with SH3 domain substitutions. Yeast strains transformed with a plasmid expressing Ark1p-GFP under control of the inducible *GAL1,10* promoter were grown in the presence of galactose for 14 hr to induce Ark1p-GFP expression. Fluorescence images of cells expressing Ark1p-GFP in the presence of wild-type Abp1p (WT) or Abp1p carrying a mutant SH3 domain (N53A, Y54A, ΔSH3) are shown. Bar, 5 μm.

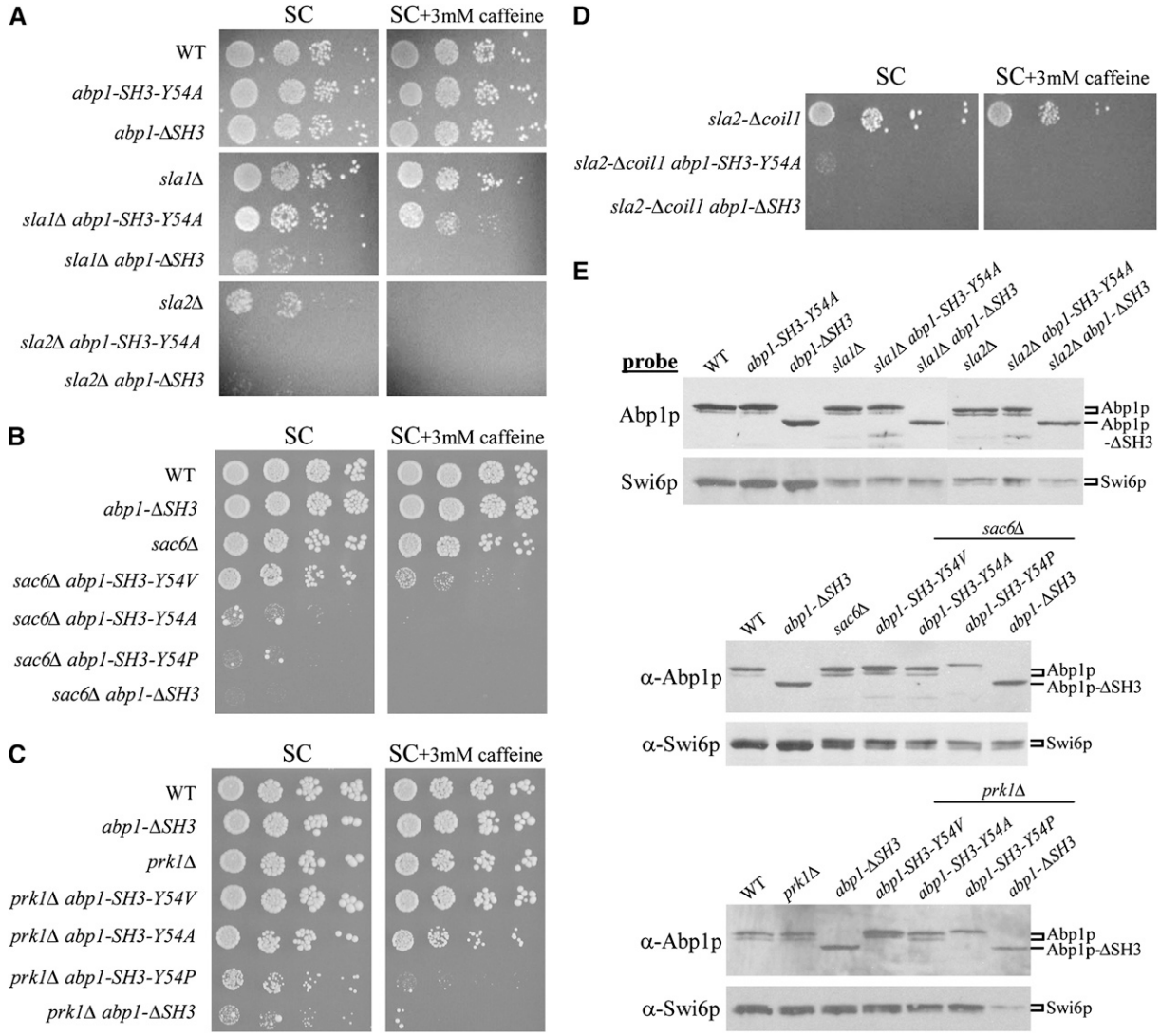

Figure 4.—Growth assays of *sla1*Δ, *sla2*, *sac6*Δ, and *prk1*Δ mutants that express different Abp1p SH3 domain derivatives. (A–D) Serial dilutions of log-phase cultures of yeast strains expressing wild-type Abp1p, Abp1p bearing a Y54 SH3 domain substitution (SH3 Y54), or Abp1p lacking an SH3 domain (ΔSH3) in the genetic background of *sla1*Δ, *sla2*Δ, *sac6*Δ, *prk1*Δ, or *sla2*-Δ*coil1* were spotted on media with or without caffeine and incubated for 3 days at 30° (*sla1*Δ, *sac6*Δ, *sla2*Δ) or 37° (*prk1*Δ, *sla2*-Δ*coil1*). *abp1* alleles were integrated at the endogenous *ABP1* locus in all mutant backgrounds, except for the *sla2*-Δ*coil1* background, for which low-copy yeast expression plasmids that contained *ABP1* coding and upstream regulatory sequences were used. (E) Western blot analysis of protein extracts prepared from strains tested for growth in A–C. Lysates were made from yeast strains expressing wild-type Abp1p, Abp1p bearing a Y54 SH3 domain substitution (SH3 Y54), or Abp1p lacking an SH3 domain (ΔSH3) in the genetic background of *sla1*Δ, *sac6*Δ, *sla2*Δ, or *prk1*Δ, which were grown to midlog phase. Protein extracts were analyzed by Western blotting using polyclonal anti-Abp1p antibody to monitor Abp1p levels or anti-Swi6p antibody to control for cellular protein levels.

was tested, as compared to N53A, is fully consistent with the >10-fold lower binding affinity of this mutant.

Viability of strains expressing Abp1p SH3 domain mutants: To investigate the consequences of reductions in Abp1p SH3 domain-binding affinity on cell viability, we examined the effect of our collection of SH3 domain mutants in four different yeast strain backgrounds in which *ABP1* is essential for cell survival. Under standard growth conditions, loss of *ABP1* alone does not confer a growth defect; however, *ABP1* encoding an intact SH3 domain is required in the absence of any one of the actin-associated genes *SLA1*, *SLA2*, or *SAC6* (Holtzman *et al.* 1993; Lila and Drubin 1997). We reiterated the synthetic growth defects of the *abp1*Δ double mutants in our laboratory strain background; however, we were able to recover slow-growing double mutants that expressed Abp1p-ΔSH3 in the absence of *SLA1*, *SLA2*, or *SAC6* when they were isolated from heterozygous diploids by tetrad dissection and allowed to grow at room temperature. These double mutants did not grow at 30°, the temperature at which our assays were performed (Figure 4, A and B). Other work has shown that *abp1*Δ has

TABLE 4

Summary of growth data for *prk1*Δ, *sla1*Δ, *sac6*Δ, and *sla2* mutants that express different Abp1p SH3 domain derivatives

Abp1p SH3 domain mutant	*prk1*Δ		*sla1*Δ		*sac6*Δ		*sla2*Δ		*sla2*-Δ*coil1*	
	SC[a]	SC + caf[b]	SC	SC + caf	SC	SC + caf	SC	SC + caf	SC	SC + caf
Wild type	++	++	++	++	++	++	+	NT[c]	++	++
N53A	++	++	++	++	++	++	+	NT	++	++
Y54V	++	++	++	++	++	+/−	+/−	NT	++	+/−
Y54A	++	+	++	+	+/−	−	−	NT	−	−
Y54P	+/−	−	+/−	−	−	−	−	NT	−	−
ΔSH3	+/−	−	+/−	−	−	−	−	NT	−	−

++, wild-type growth; +, slow; +/−, very slow; −, approximately no growth.

[a] SC, synthetic complete agar plates, incubated for 3 days at 30° (*sla1*Δ, *sac6*Δ, *sla2*Δ) or 37° (*prk1*Δ, *sla2*-Δ*coil1*).

[b] caf, 3 mM caffeine.

[c] NT, not tested; *sla2*Δ cells do not grow in this condition.

synthetic growth defects in combination with *prk1*Δ and that the resulting double mutants cannot grow at 37° (Cope *et al.* 1999). We found that the Abp1p SH3 domain was required for viability in a *prk1*Δ background at 37° (Figure 4C), and all assays with this strain were performed at this temperature.

The results of cell-spotting assays in four different actin cytoskeleton mutant backgrounds are shown in Figure 4 (see also Table 4). As expected, all double mutants that expressed Abp1p-ΔSH3 exhibited severe growth defects under standard conditions. On the other hand, expression of Abp1p carrying the N53A SH3 domain substitution was able to fully complement the *abp1*Δ synthetic growth defects under all conditions tested (Table 4; data not shown). This result is somewhat surprising as the N53A mutant showed marked reductions in its *in vitro* and *in vivo* binding to Ark1p (Table 3, Figures 2 and 3). The most striking result in these viability assays was that Abp1p carrying the Y54A SH3 domain substitution, which caused large reductions in peptide-binding activity (Table 3), displayed different phenotypes, depending on which mutant background was used. In the *sla1*Δ and *prk1*Δ backgrounds, expression of Abp1p-SH3-Y54A led to growth at a level very similar to that of wild-type Abp1p (Figure 4, A and C), whereas in the *sac6*Δ and *sla2*Δ backgrounds, double mutants that expressed Abp1p-SH3-Y54A exhibited severe growth defects (Figure 4, A and B). To assess whether the very poor growth of *sla2*Δ mutants that expressed Abp1p-SH3-Y54A was not simply due to the relatively low viability of the *sla2*Δ strain alone, we also tested mutants in a strain that contains a deletion of only a portion of *SLA2*, which is called *sla2*-Δ*coil1*. A synthetic lethal, SH3 domain-dependent growth phenotype with *ABP1* has been previously observed in this strain at 37° (Wesp *et al.* 1997). Expression of Abp1p-SH3-Y54A from a low-copy plasmid in an *abp1*Δ*sla2*-Δ*coil1* strain resulted in no growth at 37° even though expression of wild-type Abp1p leads to robust growth in this strain under these conditions (Figure 4D). Western blot analysis of total extracts showed that wild-type Abp1p and all mutants tested were present at comparable levels in all strains analyzed (Figure 4E). These data clearly illustrate that the phenotypic effect of reducing the binding affinity of the Abp1p SH3 domain can vary, depending on the mutant background of the test strain.

Previous work in our laboratory has shown a strong correlation between binding affinity of the Sho1p SH3 domain–Pbs2 interaction and biological response during activation of the Hog1 MAP kinase signal transduction pathway (Marles *et al.* 2004). To investigate the correlation between binding affinity and *in vivo* consequence for the Abp1p SH3 domain, we tested the ability of two more mutants, Y54V and Y54P, to mediate growth in *ABP1*-dependent strain backgrounds. *In vitro*, the Y54V substitution caused less severe binding defects than Y54A, while the Y54P mutant showed no detectable peptide binding (Table 3). To obtain a more nuanced picture of the effects of Abp1p SH3 mutations on growth, we also tested the double mutants when stressed by the presence of caffeine, which causes growth defects in some strains carrying mutations in genes that are important for actin cytoskeleton organization (Bach *et al.* 2000; Marcoux *et al.* 2000; Parsons *et al.* 2004). In *sac6*Δ mutants, expression of Abp1p bearing the Y54V SH3 domain substitution mediated a close to wild-type level of growth under unstressed conditions, but displayed a distinct slow-growth phenotype under stressed conditions in caffeine (Figure 4B; see also Table 4). It appears that the level of binding affinity provided by the Y54V mutant is just sufficient for growth in the *sac6*Δ background under standard conditions, but this level becomes insufficient once the cells are stressed. The Y54V mutant behaved in a very similar manner in the *sla2*Δ background (Table 4, data not shown). In contrast, Abp1p bearing the Y54V SH3 domain substitution mediated a wild-type level of growth under unstressed and stressed conditions in *prk1*Δ mutants (Figure 4C) and in *sla1*Δ mutants (data not shown). However, in both of these mutant backgrounds, expression of Abp1p-SH3-Y54A resulted in a reduction in growth under stressed conditions. Expression of Abp1p-SH3-Y54P

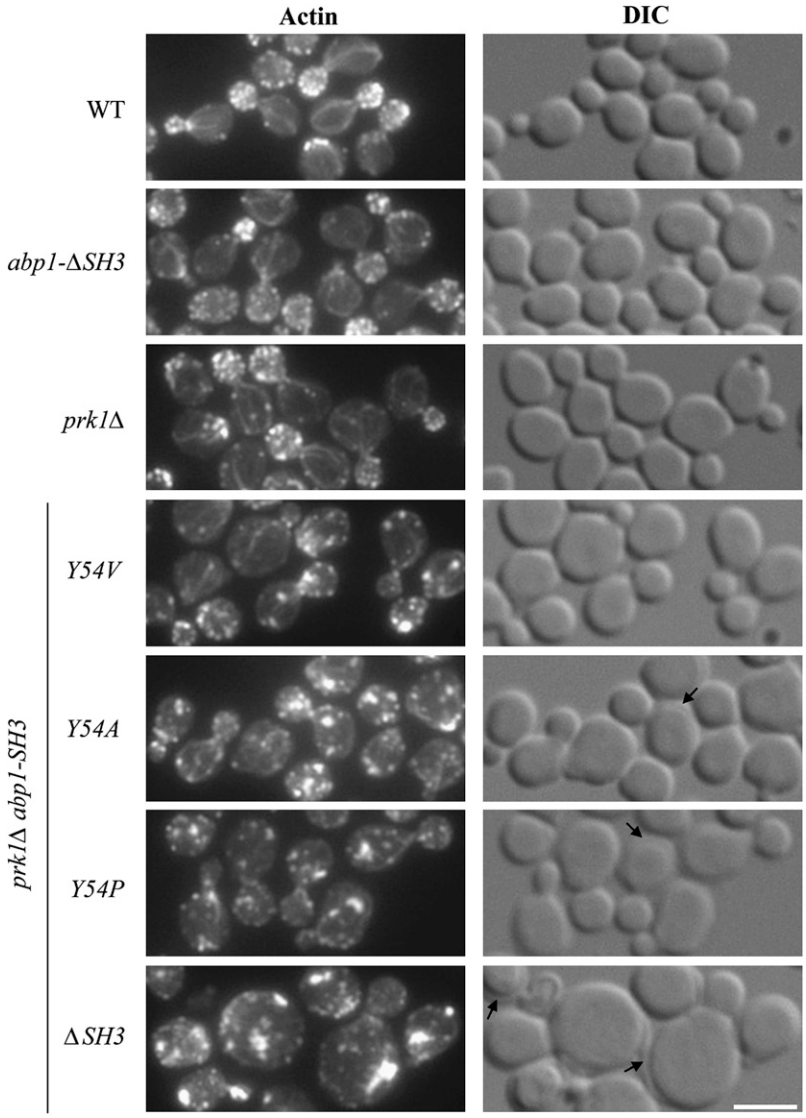

FIGURE 5.—Actin morphology of *prk1*Δ mutants that express Abp1p bearing different Y54 SH3 domain substitutions. *prk1*Δ mutants expressing wild-type Abp1p, Abp1p bearing a Y54 SH3 domain substitution (SH3 Y54), or Abp1p lacking an SH3 domain (ΔSH3) were grown to midlog phase, fixed, and stained with rhodamine-conjugated phalloidin. Actin was visualized using rhodamine fluorescence optics. Arrows indicate where the cell wall appears to have separated from the cell membrane, a cell-wall defect that is associated with cell lysis. DIC, differential interference contrast optics. Bar, 5 μm.

was unable to mediate growth under standard or stressed conditions in any of the double mutant backgrounds (Figure 4, B and C; Table 4; data not shown). These assays show that the peptide-binding activity of the Abp1p SH3 domain is definitely required for the biological activity of Abp1p, but that considerable reductions in affinity, as caused by the Y54V and Y54A substitutions, can be tolerated with little or no discernible effects on cell growth under standard conditions. In addition, the threshold K_d value at which growth defects begin to be detectable under stressed conditions varies depending on the genetic background being assayed.

The effects of Abp1p SH3 domain mutants on actin cytoskeleton organization: To determine whether mutations in the Abp1p SH3 domain that did not cause detectable changes in cell growth rates might lead to other significant biological consequences, we monitored actin cytoskeleton organization in *prk1*Δ mutants that expressed Abp1p bearing different Y54 SH3 domain substitutions. We chose to study actin defects in this mutant background because neither *abp1*Δ nor *prk1*Δ strains display any actin defects on their own, but a synthetic aberrant actin clump phenotype has been observed in *abp1*Δ*prk1*Δ double mutants (COPE *et al.* 1999). Surprisingly, rhodamine–phalloidin staining of filamentous actin revealed that expression of Abp1p bearing the Y54V SH3 domain substitution in *prk1*Δ mutants resulted in easily recognizable actin defects in >80% of small-budded cells observed (Figure 5), even though this mutant causes no effect on cell growth under any conditions tested. The observed actin defects included depolarized cortical actin patches (*i.e.*, actin patches are seen in both mother and budding daughter cells, rather than primarily localized to daughter cells) and larger aberrant actin chunks or clumps. In strains carrying only the *prk1*Δ mutation, <5% of small-budded cells displayed depolarized cortical actin patches and no cells contained actin clumps. Expression of Abp1p bearing the Y54A SH3 domain substitution in *prk1*Δ

mutants, which also leads to normal growth rates under these conditions, resulted in similar actin defects as those seen with Abp1p-SH3-Y54V, although these were more severe (Figure 5). For this double mutant strain, all cells contained both depolarized cortical patches and aberrant chunks or clumps, and there were no cells that exhibited normal actin morphology. In addition, a lysis phenotype, in which the cell wall appears to have separated from the cell membrane and mutant cell cultures exhibit increased amounts of cell lysis relative to wild-type cell cultures, was observed for *prk1*Δ mutants that expressed Abp1p-SH3-Y54A (Figure 5, right). The lysis phenotype and severe actin defects were also observed in strains that expressed Abp1p bearing the Y54P SH3 domain substitution and Abp1p-ΔSH3, as would be expected since these mutations abrogate normal growth. The only Abp1p SH3 domain substitution that caused no detectable actin defects in these experiments was N53A, which caused the smallest reduction of *in vitro* binding affinity (data not shown). The relative effects of expression of Abp1p-SH3 domain mutants on actin morphology were similar in the *sla1*Δ background (data not shown). The results of these actin morphology experiments demonstrate that the minimal binding affinity requirement of the Abp1p SH3 domain for its targets that needs to be met to support wild-type growth is different from the minimal binding affinity requirement necessary to maintain normal actin morphology.

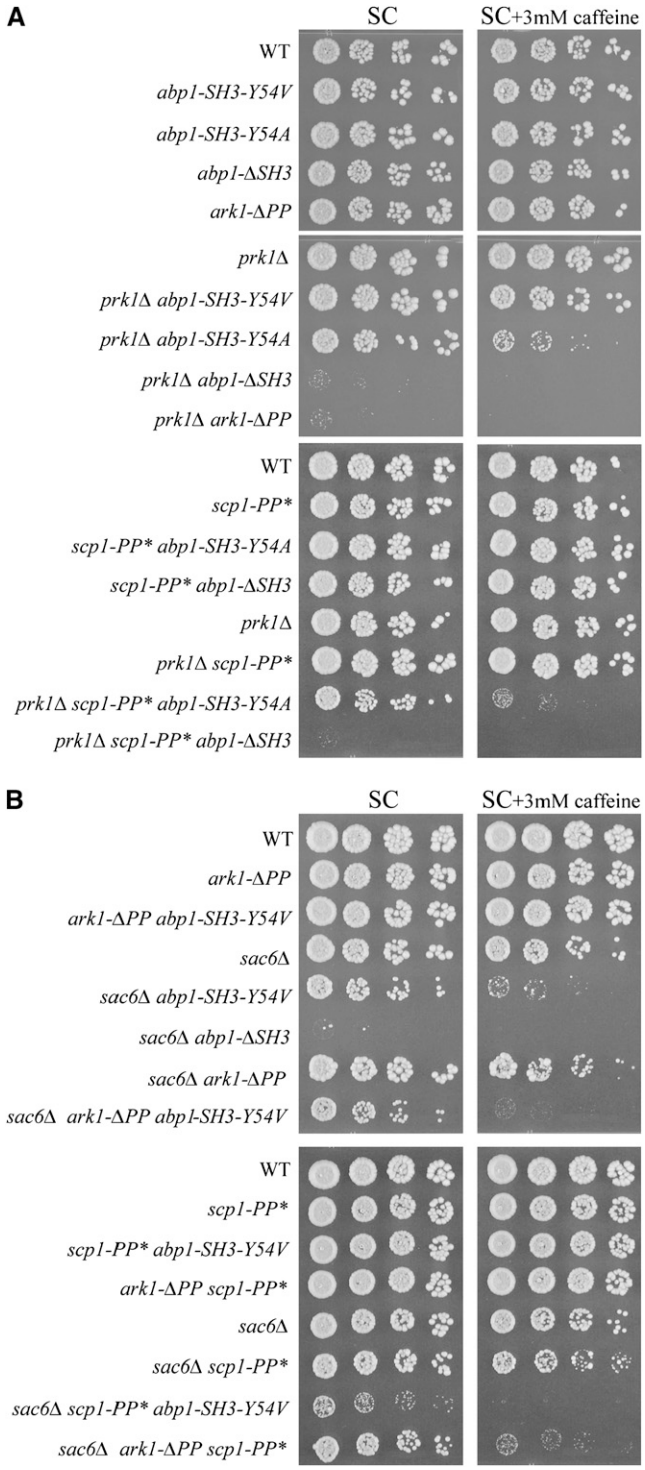

Identification of Abp1p SH3 domain-mediated interactions required for viability in the *prk1*Δ and *sac6*Δ backgrounds: To derive mechanistic explanations for the observed effects of reduced Abp1p SH3 domain-binding affinity on cell viability, it is necessary to know the relevant Abp1p SH3 domain-interacting proteins in a given strain background. Although many proteins have been identified that bind to the Abp1p SH3 domain *in vitro* and/or *in vivo* (Lila and Drubin 1997; Fazi *et al.* 2002; Landgraf *et al.* 2004; Stefan *et al.* 2005), none of these interactions has been proven to be required for normal cell viability under any condition, and the biological relevance of any specific Abp1p SH3 domain-mediated interaction has not been shown. We performed genetic studies to identify Abp1p SH3 domain-mediated interactions that are important for growth of the *prk1*Δ and *sac6*Δ backgrounds (Figure 6). Strikingly, in *prk1*Δ mutants, replacement of the wild-type *ARK1* gene with a mutant gene encoding a version of Ark1p lacking its Abp1p SH3 domain-interacting region (ΔPP mutant) (Fazi *et al.* 2002) led to significant loss of cell viability, a phenotype identical to that seen in

Figure 6.—Growth assays of *prk1*Δ and *sac6*Δ mutants that express different Abp1p SH3 domain derivatives, a mutant version of Ark1p that lacks the Abp1p SH3 domain-binding region, or a mutant version of Scp1p that has a defective Abp1p SH3 domain-binding region. Serial dilutions of log-phase cultures of yeast strains expressing wild-type Abp1p, Abp1p bearing a Y54 SH3 domain substitution (SH3 Y54), Abp1p lacking an SH3 domain (ΔSH3), Ark1p lacking an Abp1p SH3 domain-binding polyproline region (ΔPP), or Scp1p bearing a PxxP substitution in its Abp1 SH3 domain-binding polyproline region (PP*) in the genetic background of *prk1*Δ (A) or *sac6*Δ (B) were spotted on media with or without caffeine and incubated for 3 days at 37° (*prk1*Δ) or 30° (*sac6*Δ). *abp1*, *ark1*, and *scp1* alleles were integrated at the corresponding endogenous loci in all mutant backgrounds.

*prk1*Δ mutants expressing Abp1p-ΔSH3 (Figure 6A; note that the Ark1p-ΔPP mutant protein is expressed at comparable levels to wild-type Ark1p; data not shown and Fazi *et al.* 2002). This result implies that, in the *prk1*Δ background, the interaction between the Abp1p SH3 domain and Ark1p is crucial for cell growth. In a similar manner, we also tested the effect of a double point mutation constructed in the laboratory of Bruce Goode (*scp1-PP**), which abrogates the PxxP motif in the Abp1p SH3 domain-binding site of Scp1p (Figure 1B). This mutation disrupted the interaction between the Abp1p SH3 domain and Scp1p detected in a yeast two-hybrid assay (A. Goodman and B. Goode, personal communication). Expression of the Scp1p-PP* mutant in the *prk1*Δ background had no detectable effect on cell growth, indicating that binding of Scp1p by the Abp1p SH3 domain is not important for cell growth in this strain in the conditions tested here. The slight decrease in cell viability seen in the *prk1*Δ*scp1-PP* abp1-SH3-Y54A* strain as compared to the *prk1*Δ*abp1-SH3-Y54A* strain, however, does suggest a minor role for the Abp1p SH3 domain–Scp1p interaction in the *prk1*Δ background.

In contrast to the *prk1*Δ background, combining the *sac6*Δ mutation with either the *ark1-ΔPP* or the *scp1-PP** mutation produced a slight decrease in cell viability that was discernible only under stressed conditions (3 mm caffeine; Figure 6B). However, the *sac6*Δ*ark1-ΔPP scp1-PP** triple-mutant strain displayed almost no growth under stressed conditions, indicating that binding of both Ark1p and Scp1p by the Abp1p SH3 domain plays a functional role in the *sac6*Δ strain. Furthermore, the ability of the triple mutant to maintain growth under unstressed conditions while the *sac6*Δ *abp1-ΔSH3* strain cannot grow at all under these conditions suggests that the Abp1p SH3 domain makes functionally relevant interactions with at least one other protein in this strain background. It is also notable that a significant reduction in viability of the *sac6*Δ *abp1-SH3-Y54V* strain was seen in the presence of the *scp1-PP** mutation, while a much smaller effect on growth was seen when the *ark1-ΔPP* mutation was introduced into this background. This result indicates that the Abp1p SH3 domain-mediated interaction with Scp1p may be more important than that with Ark1p in the *sac6*Δ background. In total, our data clearly demonstrate that the biologically relevant targets of the Abp1p SH3 domain are different in the *prk1*Δ and *sac6*Δ backgrounds, with Ark1p being predominantly important in the *prk1*Δ strain, while Scp1p, Ark1p, and one or more other proteins play a significant role in the *sac6*Δ strain. Our experiments also show that specific mutations in the Abp1p SH3 domain and in the Abp1p-interacting region of its targets do not phenocopy deletion of the Abp1p SH3 domain, emphasizing the importance of the quantitative assessment of binding affinity mutants in exploring the function of protein modules *in vivo*.

DISCUSSION

This study has provided a detailed analysis of the correlation between changes in the *in vitro* binding activity of the Abp1p SH3 domain and its *in vivo* biological activity. We use a variety of *in vivo* tests to ask what range in binding affinities for an SH3 domain target is tolerated by the cell. In agreement with our previous study using the Sho1p SH3 domain, the severity of phenotypic defects generally increased as binding affinity was reduced. However, in contrast with the Sho1p results, we discovered that the same affinity-reducing mutation can produce a dramatically different growth phenotype, depending upon the genetic background of the strain in which it is being tested. This phenomenon is illustrated most clearly by the Abp1p-SH3-Y54A mutant, the expression of which was able to mediate cell growth at close to wild-type levels in the *prk1*Δ and *sla1*Δ backgrounds, but was unable to support cell growth in the *sac6*Δ and *sla2*Δ backgrounds (Figure 4; Table 4). These data imply that the threshold of Abp1p SH3 domain target-binding activity required for cell viability changes in these different strain backgrounds. To gain insight into the mechanisms leading to the varying Abp1p SH3 domain-binding requirements in the *prk1*Δ and *sac6*Δ backgrounds, we identified biologically relevant binding partners for this domain in these two contexts (Figure 6). Our data demonstrate that, in the *prk1*Δ background, binding of the Abp1p SH3 domain to at least one target protein, Ark1p, is crucial; whereas, in the *sac6*Δ background, elimination of the interaction with at least two target proteins (Scp1p and Ark1p) is required to produce a significant alteration in growth rate. Thus, the difference in the binding-affinity requirements for the Abp1p SH3 domain between mutant backgrounds is correlated with a change in the crucial protein–protein interaction targets.

Although our data clearly identified the Abp1p SH3 domain interactions with Ark1p and Scp1p as being important for cell viability under some conditions, we cannot rule out the importance of other putative interacting proteins (Lila and Drubin 1997; Fazi *et al.* 2002; Landgraf *et al.* 2004; Beltrao and Serrano 2005; Stefan *et al.* 2005). Here, we focused on interactions with Ark1p and Scp1p because genetic and biochemical evidence pointed to them as most likely to be biologically relevant in the *prk1*Δ and *sac6*Δ strains. In addition, previous work established that the interaction between the Abp1p SH3 domain and Srv2p was not crucial for the viability of *sac6*Δ, *sla1*Δ, or *sla2*Δ cells (Lila and Drubin 1997) and that biological effects of the interaction between the Abp1p SH3 domain and Sjl2p were detectable only in an *sjl1*Δ background (Stefan *et al.* 2005).

Our results suggest how Abp1p may contribute to multiple steps of the endocytic process through various SH3 domain-mediated interactions. We have shown that,

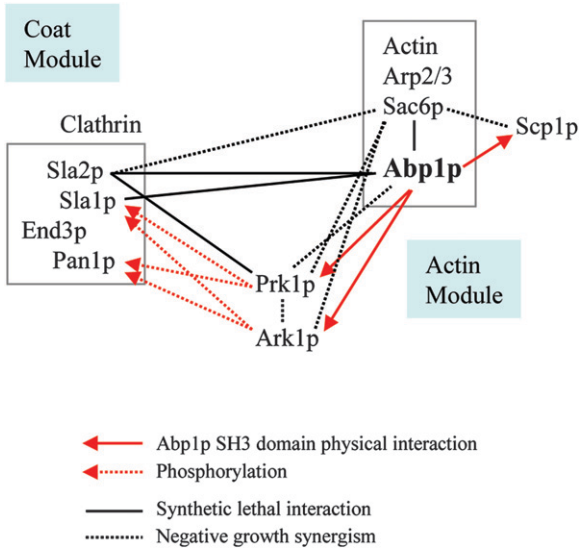

Figure 7.—A summary of synthetic genetic interactions between Abp1p SH3 domain targets and genes that are required in the absence of the Abp1p SH3 domain, which function in endocytic internalization. The "coat module" consists of a complex of endocytic coat proteins that are recruited early to endocytic sites at the plasma membrane. The "actin module" provides the actin polymerization that drives endocytic coat internalization and facilitates disassembly. Phosphorylation of coat proteins Sla1p and Pan1p by the Abp1p SH3 domain targets, Ark1p and Prk1p kinases, mediates endocytic coat protein complex disassembly.

in the absence of Prk1p, the SH3 domain-mediated interaction of Abp1p with Ark1p becomes crucial for cell viability at high temperature. This result implies that in the absence of Prk1p, the Abp1p SH3 domain is required to localize enough Ark1p to cortical actin patches/endocytic sites to adequately phosphorylate Ark1p/Prk1p substrates, including Pan1p and Sla1p, which is required for endocytic coat protein complex disassembly and for internalization to proceed (Zeng *et al.* 2001; Sekiya-Kawasaki *et al.* 2003; Toshima *et al.* 2005; Figure 7). The presence of similar large actin clumps in *prk1*Δ *abp1-SH3* mutants (Figure 5) and *prk1*Δ *ark1*Δ mutants (Cope *et al.* 1999) supports this hypothesis. Even though the Abp1p-SH3-Y54A mutant bound only weakly to the Ark1p-derived peptide *in vitro* (Table 1), did not detectably bind Ark1p in Abp1p SH3 domain affinity chromatography experiments (Figure 2), and did not visibly localize Ark1p in GFP-fusion protein localization experiments (Figure 3), *prk1*Δ strains expressing this mutant were able to grow normally under unstressed conditions (Figure 4C). Our failure to detect any association between Ark1p and the Abp1p-SH3-Y54A mutant in these and other experiments likely reflects the sensitivity of our assays and also the requirement for only a very small amount of Ark1p to be localized to cortical actin patches in the absence of Prk1p, to mediate a sufficient amount of endocytosis for cell viability. There is additional evidence that supports the view that a very low level of actin patch-associated Ark1p/Prk1p activity is required for proper function. First, endogenous levels of GFP-tagged Ark1p or Prk1p are not detectable using standard fluorescence microscopy (Cope *et al.* 1999). Second, in an otherwise wild-type background, Abp1p-ΔSH3 causes loss of detectable actin patch-associated Ark1p and Prk1p (Fazi *et al.* 2002), with no readily detectable phenotype; by contrast, *ark1*Δ*prk1*Δ cells are slow growing with obvious actin and endocytic defects.

While in the *prk1*Δ background the Abp1p SH3 domain appears to play one predominant role, we have shown that in the *sac6*Δ background it makes functionally significant interactions with both Ark1p and Scp1p. Scp1p is a member of the calponin/transgelin family that binds, crosslinks, and stabilizes actin filaments *in vitro* and shares *in vivo* functional properties with Sac6p, which is also an actin-bundling protein (Goodman *et al.* 2003; Winder *et al.* 2003). Furthermore, *sac6*Δ mutants have a synthetic growth defect in combination with *scp1*Δ, and overexpression of Scp1p can partially suppress growth defects of the *sac6*Δ strain (Goodman *et al.* 2003; Winder *et al.* 2003). Since the Abp1p SH3 domain binds to a PxxP-containing site in Scp1p (Table 3; Landgraf *et al.* 2004), it likely plays a role in localizing Scp1p to actin patches. Consistent with their common functional properties, Scp1p appears to be able to compensate for the absence of Sac6p, but it cannot do this without the participation of the Abp1p SH3 domain to facilitate its proper localization. The more stringent Abp1p SH3 domain affinity requirements in the *sac6*Δ background may be because a high concentration of Scp1p is required at actin patches. It is estimated that the actin:Sac6p:Scp1p intracellular concentration ratio is 65:6:1 (Goodman *et al.* 2003). This relatively low level of Scp1p within the cell could necessitate an efficient binding reaction with the Abp1p SH3 domain to localize enough Scp1p to actin patches for proper function. This point is emphasized by our observation that the Y54V substitution reduced the affinity of the Abp1p SH3 domain for the Scp1p-binding site by only sevenfold (Table 3), yet the *sac6*Δ *abp1-SH3-Y54V* strain displayed a marked reduction in viability under stressed conditions (Figure 4C). The sensitivity of cells to Scp1p concentrations is also emphasized by the previous finding that as little as a two- to threefold higher expression of Scp1p is sufficient to partially suppress the defects seen in *sac6*Δ cells (Goodman *et al.* 2003).

The additional requirement for Abp1p SH3 domain binding to Ark1p in *sac6*Δ cells is clearly demonstrated by the almost complete lack of growth of the *sac6*Δ *ark1-ΔPP scp1-PP** mutant under stressed conditions, as compared to the *sac6*Δ *ark1-ΔPP* and *sac6*Δ *scp1-PP** strains, which showed only subtle growth defects under these conditions. In the absence of sufficient localization and activity of Ark1p and Prk1p to mediate normal endocytic coat protein complex disassembly (Figure 7),

the defect in endocytic vesicle internalization seen in *sac6*Δ cells (Kaksonen *et al.* 2005) could lead to a complete endocytic block and detrimental amounts of actin polymerization and actin clumping, as seen in *ark1*Δ *prk1*Δ mutants (Cope *et al.* 1999; Sekiya-Kawasaki *et al.* 2003). It should be noted that since the *scp1-PP** mutant carries a double point mutation and not a complete deletion of the Abp1p SH3 domain-binding site in Scp1p, it is conceivable that this mutant retains some affinity for the Abp1p SH3 domain. Thus, the viability of some strains carrying this mutant could be partially mediated by this residual binding activity.

In light of the stunning complexity inherent in attempting to elucidate the relevant targets and functions of a protein–protein interaction domain, the determination of the *in vitro* affinities of a domain for its putative targets, and the establishment of *in vivo* affinity thresholds for the functioning of a domain, as we have done in this work, are crucial steps toward gaining a fundamental understanding of a protein–protein interaction system. Establishment of the affinity thresholds for the Abp1p SH3 domain in different backgrounds has provided clues as to which putative target proteins may be crucial in the strains where the relevant targets are still unknown. For example, Ark1p may be a crucial target for the Abp1p SH3 domain in *sla1*Δ cells, since expression of Abp1p-SH3-Y54A was able to mediate cell growth at close to wild-type levels, which is similar to the *prk1*Δ genetic background (Figure 4, A and C; Table 4). Our work has also revealed that strains that are mildly debilitated in growth due to reduced binding affinity of a domain of interest can serve as indispensable reagents for the discovery of biologically relevant binding targets. For example, elimination of binding to one relevant target protein in the *sac6*Δ strain elicited only a significant phenotype under conditions where binding affinity was limiting cell growth (*e.g.*, *sac6*Δ *scp1-PP* abp1-SH3-Y54V*; Figure 6B). A further benefit of determining affinity thresholds is that insight can be gained pertaining to the concentration of a given protein required at the site of localization. If an interaction can withstand a large reduction in affinity (*e.g.*, the Abp1p SH3 domain–Ark1p interaction), then it can be concluded that only a small amount of the target protein must be localized for adequate function (assuming that the overall concentration of the target protein within the cell is taken into account). Conversely, intolerance to affinity reductions (*e.g.*, the Abp1p SH3 domain–Scp1p interaction) is an indication that a relatively high amount of the target protein needs to be localized. In determining the mechanism of action of a given protein (*e.g.*, catalytic *vs.* structural), knowledge of the amount required for function is invaluable.

Recent live-cell imaging studies on the endocytic process emphasize the dynamic nature of this system with the key complexes being formed and then disassembled with lifetimes of <50 sec. To maintain this process at peak efficiency, individual proteins must be delivered and removed from endocytic complexes with precisely correct timing. The key role of scaffolding proteins, such as Abp1p, appears to be in facilitating the addition and removal of their binding partners in the required temporal sequence. In the absence of such proteins, the process can still occur because the machinery required is still present, but the efficiency will decrease as the timing of events is perturbed. This is reflected in significant changes in actin patch lifetimes and motilities seen when genes that are "nonessential" for the process are deleted (Kaksonen *et al.* 2003, 2005). The creation of mutants that produce defined alterations in affinities between proteins involved in dynamic processes, such as endocytosis, provides a means for altering the timing of specific events in the process as changes in affinity will also necessarily alter on and off rates. In the long-term, the establishment of correlations between changes in specific protein–protein interaction affinities and the precise dynamics of *in vivo* processes, which can now be accurately quantitated through live-cell microscopy, will provide profound insights into the mechanisms driving these processes.

We thank Bruce Goode, Anya Goodman, David Drubin, and Charlie Boone for plasmids and Bruce Goode for anti-Abp1p antibody. We are grateful to Bruce Goode and Anya Goodman for communicating unpublished results about the Abp1p SH3 domain–Scp1p interaction. We thank Mike Donoviel for construction of Abp1p yeast expression plasmid, Christine Humphries for construction of Ark1p-HA and Prk1p-HA yeast expression strains, Kasia Czarnecka for technical assistance, and Julie Forman-Kay for her support of this project. This work was supported by an operating grant from Canadian Institutes of Health Research (CIHR) to B.J.A. and A.R.D. J.H. was supported by an Estate of Betty Irene West/CIHR doctoral research award and E.J.S. was supported by a RESTRACOMP fellowship from the Hospital for Sick Children.

LITERATURE CITED

Bach, S., O. Bouchat, D. Portetelle and M. Vandenbol, 2000 Co-deletion of the MSB3 and MSB4 coding regions affects bipolar budding and perturbs the organization of the actin cytoskeleton. Yeast **16:** 1015–1023.

Beltrao, P., and L. Serrano, 2005 Comparative genomics and disorder prediction identify biologically relevant SH3 protein interactions. PLoS Comput. Biol. **1:** e26.

Brachmann, C. B., A. Davies, G. J. Cost, E. Caputo, J. Li *et al.*, 1998 Designer deletion strains derived from Saccharomyces cerevisiae S288C: a useful set of strains and plasmids for PCR-mediated gene disruption and other applications. Yeast **14:** 115–132.

Cope, M. J., S. Yang, C. Shang and D. G. Drubin, 1999 Novel protein kinases Ark1p and Prk1p associate with and regulate the cortical actin cytoskeleton in budding yeast. J. Cell Biol. **144:** 1203–1218.

Drubin, D. G., 1990 Actin and actin-binding proteins in yeast. Cell Motil. Cytoskeleton **15:** 7–11.

Drubin, D. G., K. G. Miller and D. Botstein, 1988 Yeast actin-binding proteins: evidence for a role in morphogenesis. J. Cell Biol. **107:** 2551–2561.

Engqvist-Goldstein, A. E., and D. G. Drubin, 2003 Actin assembly and endocytosis: from yeast to mammals. Annu. Rev. Cell Dev. Biol. **19:** 287–332.

Fazi, B., M. J. Cope, A. Douangamath, S. Ferracuti, K. Schirwitz *et al.*, 2002 Unusual binding properties of the SH3 domain of the yeast actin-binding protein Abp1: structural and functional analysis. J. Biol. Chem. **277:** 5290–5298.

Friesen, H., K. Murphy, A. Breitkreutz, M. Tyers and B. Andrews, 2003 Regulation of the yeast amphiphysin homologue Rvs167p by phosphorylation. Mol. Biol. Cell **14:** 3027–3040.

Friesen, H., K. Colwill, K. Robertson, O. Schub and B. Andrews, 2005 Interaction of the *Saccharomyces cerevisiae* cortical actin patch protein Rvs167p with proteins involved in ER to Golgi vesicle trafficking. Genetics **170:** 555–568.

Gavin, A. C., M. Bosche, R. Krause, P. Grandi, M. Marzioch *et al.*, 2002 Functional organization of the yeast proteome by systematic analysis of protein complexes. Nature **415:** 141–147.

Goode, B. L., A. A. Rodal, G. Barnes and D. G. Drubin, 2001 Activation of the Arp2/3 complex by the actin filament binding protein Abp1p. J. Cell Biol. **153:** 627–634.

Goodman, A., B. L. Goode, P. Matsudaira and G. R. Fink, 2003 The Saccharomyces cerevisiae calponin/transgelin homolog Scp1 functions with fimbrin to regulate stability and organization of the actin cytoskeleton. Mol. Biol. Cell **14:** 2617–2629.

Guthrie, C., and G. R. Fink, 1991 *Guide to Yeast Genetics and Molecular Biology*. Academic Press, San Diego.

Ho, Y., A. Gruhler, A. Heilbut, G. D. Bader, L. Moore *et al.*, 2002 Systematic identification of protein complexes in Saccharomyces cerevisiae by mass spectrometry. Nature **415:** 180–183.

Holtzman, D. A., S. Yang and D. G. Drubin, 1993 Synthetic-lethal interactions identify two novel genes, SLA1 and SLA2, that control membrane cytoskeleton assembly in Saccharomyces cerevisiae. J. Cell Biol. **122:** 635–644.

Kaksonen, M., Y. Sun and D. G. Drubin, 2003 A pathway for association of receptors, adaptors, and actin during endocytic internalization. Cell **115:** 475–487.

Kaksonen, M., C. P. Toret and D. G. Drubin, 2005 A modular design for the clathrin- and actin-mediated endocytosis machinery. Cell **123:** 305–320.

Landgraf, C., S. Panni, L. Montecchi-Palazzi, L. Castagnoli, J. Schneider-Mergener *et al.*, 2004 Protein interaction networks by proteome peptide scanning. PLoS Biol. **2:** E14.

Larson, S. M., and A. R. Davidson, 2000 The identification of conserved interactions within the SH3 domain by alignment of sequences and structures. Protein Sci. **9:** 2170–2180.

Lee, J., K. Colwill, V. Aneliunas, C. Tennyson, L. Moore *et al.*, 1998 Interaction of yeast Rvs167 and Pho85 cyclin-dependent kinase complexes may link the cell cycle to the actin cytoskeleton. Curr. Biol. **8:** 1310–1321.

Li, S., C. M. Armstrong, N. Bertin, H. Ge, S. Milstein *et al.*, 2004 A map of the interactome network of the metazoan C. elegans. Science **303:** 540–543.

Lila, T., and D. G. Drubin, 1997 Evidence for physical and functional interactions among two Saccharomyces cerevisiae SH3 domain proteins, an adenylyl cyclase-associated protein and the actin cytoskeleton. Mol. Biol. Cell **8:** 367–385.

Longtine, M. S., A. McKenzie, III, D. J. Demarini, N. G. Shah, A. Wach *et al.*, 1998 Additional modules for versatile and economical PCR-based gene deletion and modification in Saccharomyces cerevisiae. Yeast **14:** 953–961.

Marcoux, N., S. Cloutier, E. Zakrzewska, P. M. Charest, Y. Bourbonnais *et al.*, 2000 Suppression of the profilin-deficient phenotype by the RHO2 signaling pathway in *Saccharomyces cerevisiae*. Genetics **156:** 579–592.

Marles, J. A., S. Dahesh, J. Haynes, B. J. Andrews and A. R. Davidson, 2004 Protein-protein interaction affinity plays a crucial role in controlling the sho1p-mediated signal transduction pathway in yeast. Mol. Cell **14:** 813–823.

Mattila, P. K., O. Quintero-Monzon, J. Kugler, J. B. Moseley, S. C. Almo *et al.*, 2004 A high-affinity interaction with ADP-actin monomers underlies the mechanism and in vivo function of Srv2/cyclase-associated protein. Mol. Biol. Cell **15:** 5158–5171.

Mayer, B. J., 2001 SH3 domains: complexity in moderation. J. Cell Sci. **114:** 1253–1263.

Measday, V., L. Moore, J. Ogas, M. Tyers and B. Andrews, 1994 The PCL2 (ORFD)-PHO85 cyclin-dependent kinase complex: a cell cycle regulator in yeast. Science **266:** 1391–1395.

Measday, V., L. Moore, R. Retnakaran, J. Lee, M. Donoviel *et al.*, 1997 A family of cyclin-like proteins that interact with the Pho85 cyclin-dependent kinase. Mol. Cell. Biol. **17:** 1212–1223.

Mulholland, J., D. Preuss, A. Moon, A. Wong, D. Drubin *et al.*, 1994 Ultrastructure of the yeast actin cytoskeleton and its association with the plasma membrane. J. Cell Biol. **125:** 381–391.

Newpher, T. M., R. P. Smith, V. Lemmon and S. K. Lemmon, 2005 In vivo dynamics of clathrin and its adaptor-dependent recruitment to the actin-based endocytic machinery in yeast. Dev. Cell **9:** 87–98.

Ogas, J., B. J. Andrews and I. Herskowitz, 1991 Transcriptional activation of CLN1, CLN2, and a putative new G1 cyclin (HCS26) by SWI4, a positive regulator of G1-specific transcription. Cell **66:** 1015–1026.

Parsons, A. B., R. L. Brost, H. Ding, Z. Li, C. Zhang *et al.*, 2004 Integration of chemical-genetic and genetic interaction data links bioactive compounds to cellular target pathways. Nat. Biotechnol. **22:** 62–69.

Pawson, T., and J. D. Scott, 1997 Signaling through scaffold, anchoring, and adaptor proteins. Science **278:** 2075–2080.

Rath, A., and A. R. Davidson, 2000 The design of a hyperstable mutant of the Abp1p SH3 domain by sequence alignment analysis. Protein Sci. **9:** 2457–2469.

Ren, R., B. J. Mayer, P. Cicchetti and D. Baltimore, 1993 Identification of a ten-amino acid proline-rich SH3 binding site. Science **259:** 1157–1161.

Rual, J. F., K. Venkatesan, T. Hao, T. Hirozane-Kishikawa, A. Dricot *et al.*, 2005 Towards a proteome-scale map of the human protein-protein interaction network. Nature **437:** 1173–1178.

Sekiya-Kawasaki, M., A. C. Groen, M. J. Cope, M. Kaksonen, H. A. Watson *et al.*, 2003 Dynamic phosphoregulation of the cortical actin cytoskeleton and endocytic machinery revealed by real-time chemical genetic analysis. J. Cell Biol. **162:** 765–772.

Sikorski, R. S., and P. Hieter, 1989 A system of shuttle vectors and yeast host strains designed for efficient manipulation of DNA in *Saccharomyces cerevisiae*. Genetics **122:** 19–27.

Stefan, C. J., S. M. Padilla, A. Audhya and S. D. Emr, 2005 The phosphoinositide phosphatase Sjl2 is recruited to cortical actin patches in the control of vesicle formation and fission during endocytosis. Mol. Cell. Biol. **25:** 2910–2923.

Tong, A. H., M. Evangelista, A. B. Parsons, H. Xu, G. D. Bader *et al.*, 2001 Systematic genetic analysis with ordered arrays of yeast deletion mutants. Science **294:** 2364–2368.

Toshima, J., J. Y. Toshima, A. C. Martin and D. G. Drubin, 2005 Phosphoregulation of Arp2/3-dependent actin assembly during receptor-mediated endocytosis. Nat. Cell Biol. **7:** 246–254.

Warren, D. T., P. D. Andrews, C. W. Gourlay and K. R. Ayscough, 2002 Sla1p couples the yeast endocytic machinery to proteins regulating actin dynamics. J.Cell Sci. **115:** 1703–1715.

Wesp, A., L. Hicke, J. Palecek, R. Lombardi, T. Aust *et al.*, 1997 End4p/Sla2p interacts with actin-associated proteins for endocytosis in Saccharomyces cerevisiae. Mol. Biol. Cell **8:** 2291–2306.

Winder, S. J., T. Jess and K. R. Ayscough, 2003 SCP1 encodes an actin-bundling protein in yeast. Biochem. J. **375:** 287–295.

Winzeler, E. A., D. D. Shoemaker, A. Astromoff, H. Liang, K. Anderson *et al.*, 1999 Functional characterization of the S. cerevisiae genome by gene deletion and parallel analysis. Science **285:** 901–906.

Zeng, G., X. Yu and M. Cai, 2001 Regulation of yeast actin cytoskeleton-regulatory complex Pan1p/Sla1p/End3p by serine/threonine kinase Prk1p. Mol. Biol. Cell **12:** 3759–3772.

Communicating editor: M. D. Rose